A Multicriteria Approach for the Integration of Renewable Energy Technologies and Thermal Energy Storage to Support Building Trigeneration Systems

Eduardo A. Pina, Miguel A. Lozano, Luis M. Serra

GITSE-I3A, Department of Mechanical Engineering, University of Zaragoza, Zaragoza (Spain)

Abstract

Trigeneration systems benefit from process integration to achieve primary energy savings, reduction of pollutant emissions, and reduction of unit costs relative to conventional separate production. Achieving such benefits requires an appropriate design procedure. The issue is that finding the best configuration that minimizes total annual cost is not enough anymore, as the environmental concern has become an ever-present theme in the design and synthesis of energy systems. The minimization of costs is often contradictory to the minimization of environmental impact. Multiobjective optimization tackles the issue of conflicting objectives by providing a set of trade-off solutions, or Pareto solutions, that can be examined by the decision maker, so that the best configuration can be selected for a given scenario. This paper proposes a mixed integer linear programming model (MILP) to determine the optimal configuration and hourly operation of trigeneration systems considering the effects of thermal energy storage (TES) and hourly variations of solar radiation, energy supply prices, energy demands, and CO_2 emissions. The objective functions to be minimized are the total annual costs and the total annual CO_2 emissions. Initially, the objective functions were evaluated separately. Then, the Pareto curve was obtained for the minimization of total annual cost subject to CO_2 emissions restrictions. The trade-off solutions were analyzed and the preferred solutions were selected, achieving results close to the optimal solutions with reasonable sacrifices for both objectives.

Keywords: buildings, multicriteria, photovoltaics, solar thermal energy, thermal energy storage, trigeneration.

1. Introduction

Environmental awareness, depletion of fossil fuels resources, and economic aspects are some of the factors that motivate the development of alternative energy systems. Process energy integration is regarded as an effective way to achieve primary energy savings and reduction of pollutant emissions relative to conventional separate production (Mancarella, 2014; Serra et al., 2009). Trigeneration systems benefit from process integration, producing electricity (and/or mechanical energy), heating, and cooling from a common resource. There is a large potential for the incorporation of trigeneration systems in the residential-commercial sector (Liu et al., 2014; Rong and Su, 2017).

In the design of trigeneration plants, two fundamental issues must be addressed (Lozano et al., 2009; Wakui et al., 2016): the synthesis of the plant configuration (installed technologies and capacities, etc.) and the operational planning (strategy concerning the operational state of the equipment, energy flow rates, purchase/selling of electricity, etc.). Finding the optimal configuration of trigeneration systems in building applications is a complex task, given the wide variety of technology options available and great diurnal and annual fluctuations in energy demands and energy prices. Other factors that further increase complexity are: (i) the incorporation of renewable energy technologies, such as photovoltaic panels and solar thermal collectors, which are characterized by intermittent behavior and non-simultaneity between production and consumption; (ii) the incorporation of TES units, which allow to decouple production from consumption; and (iii) conflicting objectives, as the minimization of environmental burdens is often contradictory to the minimization of costs.

Nowadays, sustainability-related issues are ever-present themes in the design of energy systems. Therefore, a purely economic analysis is not sufficient anymore. Multiobjective optimization tackles the issue of conflicting objectives by providing a set of non-dominated solutions (Pareto Frontier), which provides flexibility and allows the decision maker's judgement into the optimization problem (Andiappan, 2017).

doi:10.18086/swc.2017.10.03 Available at http://proceedings.ises.org

One of the most important steps in the optimization problem is data collection, since the quality of the data given as input to the model will directly affect the results obtained. In this regard, it is essential to maintain the same level of detail for all aspects of the model; however, this information is not always easily obtained or identified. In the case of hourly optimization problems, Pina et al. (2017) argued the difficulty of finding hourly CO_2 emissions data associated with the electricity available in the Spanish electric grid, as opposed to the well-established hourly electricity prices. Because the authors could not find appropriate CO_2 emissions data on an hourly basis, a constant annual average was considered; as a result, it was necessary to consider a constant electricity price as well, as it is not consistent to evaluate electricity prices on an hourly basis and electricity CO_2 emissions on a constant annual value.

This work improves the optimization model proposed by Pina et al. (2017) to include hourly electricity prices and the corresponding hourly CO_2 emissions, instead of constant annual values. The MILP model determines the optimal configuration and optimal operation of trigeneration systems, considering the effects of thermal energy storage and hourly variations of solar radiation, energy supply prices, energy demands, and CO_2 emissions associated with the electricity from the electric grid. A multiobjective optimization procedure is presented, taking into consideration the minimization of the total annual cost and total annual CO_2 emissions. The MILP model provides a Pareto frontier, a set of solutions representing the optimal trade-offs between the economic and environmental objectives, in which there can be no increase in one objective without a decrease in the value of the other. The solutions along the Pareto curve were analyzed and the preferred trade-off solutions were selected.

2. Solar assisted trigeneration system

The synthesis of trigeneration systems begins with the definition of a superstructure (Iyer and Grossmann, 1998; Lozano et al., 2010; Yokoyama et al., 2015). The first step in defining the superstructure is to identify design targets, that is, the types and quantities of resources available (e.g. fuels, electricity from the electric grid) and desired products (energy demands of the consumer center that the system must attend), as well as possible restrictions (e.g. permission or not to sell electricity to the grid). Then, the superstructure can be established, considering potential technologies and the feasible connections between them, based on appropriate process integration. Once the superstructure is defined, additional and more specific data are incorporated; this step plays an essential role, since the quality of the data collected will directly affect the results of the optimization model. After the optimization procedure, the superstructure will be reduced to its optimal configuration. These three steps are presented in the following subsections.

2.1. Energy demands

The consumer center considered in this study is a multifamily building located in Zaragoza, Spain. The complex is composed of 100 dwellings, each one with 100 m² surface area. The energy demands of the consumer center are assumed to be known beforehand: the annual electricity, heating, and cooling demands are 254,963 kWh, 573,503 kWh, and 113,989 kWh, respectively. The electricity demand is required all year round. The heating demand is composed of domestic hot water, required all through the year, and space heating, required from November to April. The cooling demand is only required in the summer months (from June to September).

The study covers the period of one year. It was considered that the energy demands and the operation of the system are described by 12 representative days d (NRD = 12) each one composed of 24 consecutive periods h (NP = 24) of 1-hour duration ($NHP(h)$ = 1). Each representative day d is attributed to a month of the year, so the number of representative days d per year is equal to the number of days in the corresponding month ($NRY(1, 2, 3, \ldots, 12)$ = 31, 28, 31, …, 31). Two additional representative days were included to account for extreme demand situations, as described in Pina et al. (2017); what these extreme representative days do is increase the technologies' installed capacity for safety power margin, with impact on the annual fixed cost, but not on the annual operation cost.

2.2. Superstructure

The superstructure of the trigeneration system considered in this study is depicted in Fig. 1. Natural gas F_p, electricity purchased from the grid E_p, and solar radiation F_{pv} and F_{st} are the resources that can be used by the system to attend the electricity E_d, heating Q_d, and cooling R_d demands of the consumer center. Heat can be

produced at two temperature levels: low-temperature heat is only used to cover the heating demand, while high-temperature heat can also be used for cooling production. The cogeneration module GE (natural gas reciprocating engine coupled to a heat recovery system) consumes natural gas F_c and produces electricity W_c, low-temperature heat Q_{cc}, and high-temperature heat Q_{cr}; also, a portion of the total heat produced can be dissipated to the environment Q_{cl}. The gas boiler GB consumes natural gas F_a and produces low-temperature heat Q_{ac} and high-temperature heat Q_{ar}. The photovoltaic panels PV produce electricity W_{pv} from the incident solar radiation F_{pv}. The single-effect absorption chiller ABS uses high-temperature heat Q_{abs} to produce cooling R_{abs}; this technology also consumes a small quantity of electricity W_{abs}. The reversible heat pump HP and the solar thermal collectors ST are assumed to operate in two operation modes according to the month of the year:

- From January to May and from October to December: The HP operates in heating mode (HPQ), consuming electricity W_{hp} to produce low-temperature heat Q_{hp}. The ST produces low-temperature heat Q_{stc} from the incident solar radiation F_{st};
- From June to September: The HP operates in cooling mode (HPR), consuming electricity W_{hp} to produce cooling R_{hp}. The ST can produce low and/or high-temperature heat Q_{stc} and Q_{str}, respectively.

Both operation modes consider the possibility of dissipating heat from the ST Q_{stl}. Finally, two thermal energy storage tanks are considered, one for low-temperature heat (TSQ) and another for cooling (TSR). Energy can be charged to/discharged from the TSQ Q_{in}/Q_{out} and TSR R_{in}/R_{out}. Energy losses Q_s and R_s are proportional to the stored energy S_q and S_r, respectively, and to an hourly energy loss factor.

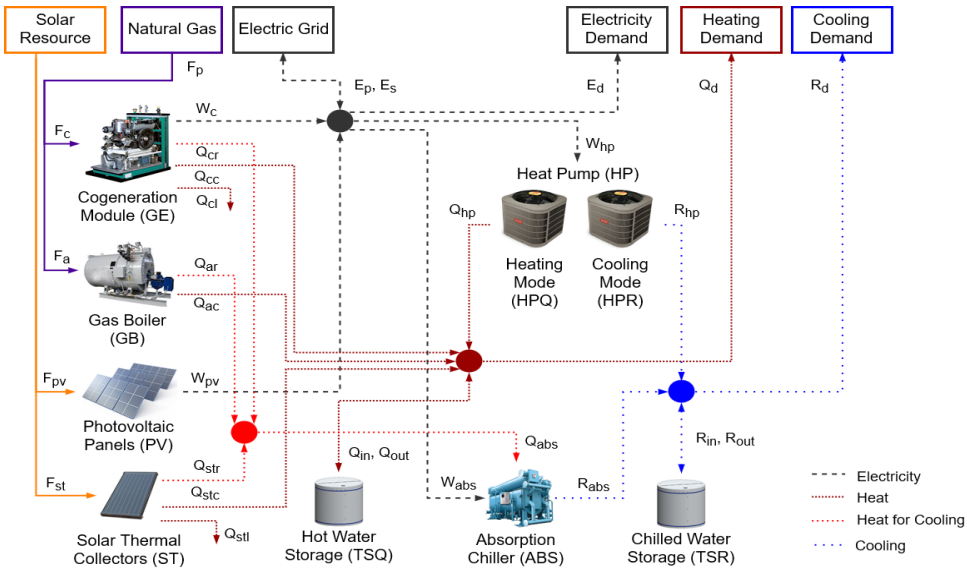

Fig. 1: Superstructure of the trigeneration system

2.3. Data collection and elaboration

Once the superstructure is established, it is necessary to provide more specific information about the system in line with the objective of the analysis. In this regard, in order to contemplate the technical, economic, and environmental aspects of the incorporation of potentially installable technologies, including renewable energy technologies and thermal energy storage units, in the building trigeneration system analyzed herein, the following information is required:

(i) Technical data

All technologies included in the superstructure are commercially available. The equipment can modulate up to nominal load, except for the non-manageable ones (PV and ST). Performance variations with ambient and operation conditions are taken into consideration. Table 1 presents the technologies' main technical parameters obtained from the manufacturers' catalogs. The PV has a maximum power of 0.260 kW, module efficiency of 15.51%, and total surface area of 1.60 m². The ST presents thermal performances of k_0 = 0.789, k_1 = 3.834 W/(m²·K), and k_2 = 0.011 W/(m²·K²), and total surface area of 5.04 m². The hourly unit productions per square

meter of the PV panels and ST collectors were evaluated as explained in Pina et al. (2017).

Table 1: Technologies' technical parameters

Parameter	Value	Parameter	Value
GE Electric power efficiency, α_w	0.26	HP Cooling/heating capacity ratio, *RCAPrq*	0.90
GE Thermal efficiency, α_q	0.61	ABS COP, *COPabs*	0.69
GB Thermal efficiency, η_q	0.95	ABS unit electricity consumption, *kwabs*	0.03
HP COP in heating mode, *COPhpq*	3.24	TSQ hourly energy loss factor, *fpacuQ*	0.01
HP COP in cooling mode, *COPhpr*	3.19	TSR hourly energy loss factor, *fpacuR*	0.01

Based on the geometry of the buildings, a total roof top area of 2000 m² is available for the installation of PV panels and ST collectors. PV and ST are installed with a tilt of 35º and 30º, respectively. Considering their surface areas and tilt, it was possible to determine the roof top area occupied by each square meter of PV and ST: the PV unit surface area usage is equal to 3.1250 m² roof/m² PV and the ST unit surface area usage is equal to 2.2676 m² roof/m² ST.

(ii) Economic data

Table 2 presents the unit investment cost *CI* of each technology *i* included in the superstructure. These values were obtained from manufacturers' catalogs (including taxes) and multiplied by a simple module factor that took into account transportation, installation, connection costs, etc. An operational lifetime *nyr* of 20 years was considered for all equipment. An amortization and maintenance factor *fam* of 0.15 yr^{-1} and an indirect costs factor *fic* of 0.20 were considered (Ramos, 2012).

Table 2: Technologies' economic and environmental data

Technology *i*	Unit Investment cost *CI*	Unit CO_2 emissions *CO2U*	Technology *i*	Unit Investment cost *CI*	Unit CO_2 emissions *CO2U*
GE	2700 €/kW_{el}	65 kg CO_2/kW_{el}	PV	264 €/m²	285 kg CO_2/m²
GB	77 €/kW_{th}	10 kg CO_2/kW_{th}	ST	578 €/m²	95 kg CO_2/m²
HP	481 €/kW_{th}	160 kg CO_2/kW_{th}	STQ	150 €/kWh	150 kg CO_2/kWh
ABS	518 €/kW_{th}	165 kg CO_2/kW_{th}	STR	300 €/kWh	300 kg CO_2/kWh

Gas and electricity rates were taken from a real Spanish distributor (EDP, 2017). The gas price is constant all through the year c_g = 0.057 €/kWh LHV (with taxes). In the case of the electricity purchase price c_{ep}, a time-of-use tariff is applied with three time periods, namely on-peak, mid-peak, and off-peak, whose rates are given in Table 3. The selling price of electricity c_{es} was assumed to be the same as the purchase price c_{ep}.

Table 3: Electricity prices in €/kWh, with taxes (EDP, 2017)

Annual period	On-peak		Mid-peak		Off-peak	
	Hours	c_{ep}	Hours	c_{ep}	Hours	c_{ep}
Winter (Jan-Mar, Nov-Dec)	19-22	0.183	9-18, 23-24	0.156	1-8	0.122
Summer (Apr-Oct)	12-15	0.183	9-11, 16-24	0.156	1-8	0.122

(iii) Environmental data

Table 2 presents the unit CO_2 emissions *CO2U* of each technology *i* of the superstructure. The *CO2U* values were obtained from the literature (Carvalho, 2011; Guadalfajara, 2016; Ito et al., 2009; Ralui et al., 2014).

In terms of CO_2 emissions, the environmental cost associated with the consumption of natural gas is constant throughout the year *kgCO2g* = 0.252 kg CO_2/kWh; this is a Spanish national value obtained from IDAE (2014). *Red Eléctrica de España* (REE, 2017) provides data on the national electric demand, generation, and associated emissions on a 10-minute basis. We have processed this information to obtain the hourly CO_2 emissions associated with the electricity available in the grid for each representative day, as shown in Fig. 2.

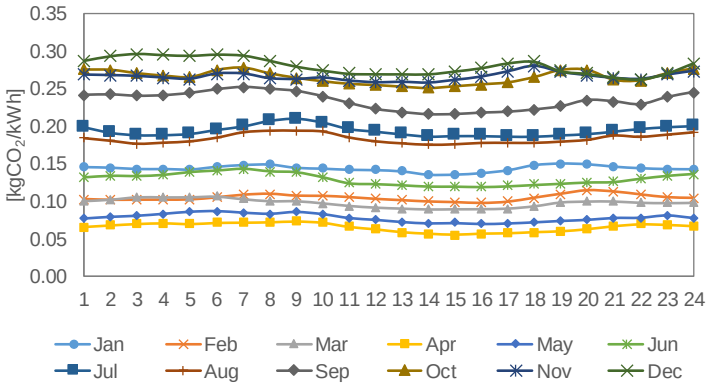

Fig. 2: Hourly CO_2 emissions of the electricity in Spain for each representative day, in kg CO_2/kWh (REE, 2017)

3. Mathematical model

Having defined the superstructure of the trigeneration system, it is necessary to develop a mathematical model, representing the behavior and performances of all elements in the superstructure, to determine the optimal configuration and optimal operation modes of the system. A MILP model was developed using the software LINGO (Schrage, 1999). Two objective functions are included: the first considers the economic aspects of the trigeneration system through the total annual cost, while the second considers the environmental impact in terms of the total annual CO_2 emissions.

The economic objective is to minimize the total annual cost C_{tot}, which consists of the annual fixed cost C_{fix} and the annual operation cost C_{ope}.

$$Min\ C_{tot} = C_{fix} + C_{ope} \tag{1}$$

The annual fixed cost is expressed by Eq. (2)

$$C_{fix} = fam \cdot (1 + fic) \cdot \sum_i CI(i) \cdot CAP(i) \tag{2}$$

in which the *fam*, *fic*, and *CI* were given in Section 2 (*CI* values are given in Table 2).

As explained earlier, it was considered that the year was divided into *NRD* representative days *d*, each one composed of *NP* consecutive hourly periods *h* of *NHP(h)* duration. Throughout the year there are *NRY(d)* days for each representative day type *d*. The annual operation cost includes fuel costs and the purchase/sale of electricity, as expresses Eq. (3):

$$C_{ope} = \sum_{d=1}^{NRD} \sum_{h=1}^{NP} NRY(d) \cdot NHP(h) \cdot \left(F_p(d,h) \cdot c_g + E_p(d,h) \cdot c_{ep}(d,h) - E_s(d,h) \cdot c_{es}(d,h)\right) \tag{3}$$

Regarding the environmental objective, the goal is to minimize the total annual CO_2 emissions $CO2_{tot}$, which is composed of the annual fixed emissions $CO2_{fix}$ and the annual operation emissions $CO2_{ope}$.

$$Min\ CO2_{tot} = CO2_{fix} + CO2_{ope} \tag{4}$$

The annual fixed emissions, annualized for the equipment's operational lifetime *nyr* is expressed by Eq. (5)

$$CO2_{fix} = \sum_i CO2U(i) \cdot CAP(i)/nyr \tag{5}$$

in which the *CO2U* values of each technology *i* are given in Table 2.

The annual CO_2 emissions associated with the operation of the system is expressed by Eq. (6). The first and second terms within the parenthesis correspond to the emissions associated with the purchase of natural gas and electricity, respectively, while the last term corresponds to the avoided emissions due to the selling of electricity.

$$CO2_{ope} = \sum_{d=1}^{NRD} \sum_{h=1}^{NP} NRY(d) \cdot NHP(h) \cdot \left(F_p(d,h) \cdot kgCO2_g + E_p(d,h) \cdot kgCO2_e(d,h) - E_s(d,h) \cdot kgCO2_e(d,h)\right) \quad (6)$$

The objective functions are subject to equipment constraints (capacity limits and production restrictions), balance equations, and electric grid constraints (permission to purchase/sell electricity). The reader is referred to Pina et al. (2017) for a detailed explanation of the restrictions.

4. Single-objective optimization

The two objective functions were initially evaluated separately. Table 4 gathers the main results obtained for the minimization of total annual costs and total annual CO_2 emissions.

For the optimal annual cost solution, all candidate technologies were included except for the PV and ST; further, the TSQ installed capacity is so small (0.4 kWh) that it could be dropped out. Regarding the annual investment cost, 47% is due to the installation of HP, followed by the ABS with 29%, and the GB with 10%. Taking into account the annual CO_2 emissions relative to the manufacturing of each device, the HP also accounts for the highest share, 46%, followed by the ABS with 28%, and the TSR with 21%. This configuration heavily relies on natural gas (363,285 kWh/yr) and electricity from the electric grid (355,040 kWh/yr). Further, all electricity produced by the GE is consumed, so that there is no selling.

Table 4: Main results of the single-objective solutions

Technology	Optimal annual cost (B)			Optimal annual CO_2 emissions (A)		
	Installed capacity	**Investment cost [€/yr]**	**CO_2 emissions [kgCO_2/yr]**	**Installed capacity**	**Investment cost [€/yr]**	**CO_2 emissions [kgCO_2/yr]**
GE	4.2 kW_{el}	2050.8	13.7	0.0 kW_{el}	-	-
GB	204.8 kW_{th}	2838.1	102.4	49.3 kW_{th}	683.1	24.6
HP	162.1 kW_{th}	14,031.7	1296.5	269.6 kW_{th}	23,343.1	2156.9
ABS	94.0 kW_{th}	8761.6	775.2	48.8 kW_{th}	4554.4	403.0
PV	0.0 m²	-	-	461.2 m²	21,873.1	6571.6
ST	0.0 m²	-	-	246.5 m²	25,618.8	1170.7
TSQ	0.4 kWh	10.8	3.0	314.0 kWh	8449.1	2354.8
TSR	39.9 kWh	2148.9	598.9	0.0 kWh	-	-
Annual fixed	C_{fix} / $CO2_{fix}$	29,841.9	2789.8		84,521.6	12,681.6
Energy service	**Consumption [kWh/yr]**	**Energy cost [€/yr]**	**CO_2 emissions [kgCO_2/yr]**	**Consumption [kWh/yr]**	**Energy cost [€/yr]**	**CO_2 emissions [kgCO_2/yr]**
Natural gas	363,285.1	20,557.7	91,547.8	124.2	7.0	31.3
Purchased electricity	355,040.0	54,667.3	60,728.1	355,919.7	54,606.8	63,048.5
Sold electricity	-	-	-	9348.0	1505.1	1521.3
Annual operation C_{ope} / $CO2_{ope}$		75,225.0	152,275.9		53,108.7	61,558.5
Total annual C_{tot} / $CO2_{tot}$		**105,066.9 €/yr**	155,065.7 kgCO_2/yr		137,630.2 €/yr	**74,240.1 kgCO_2/yr**

In the case of the optimal annual CO_2 emissions solution, all technologies were included except for the GE and TSR. Compared with the optimal annual cost configuration, the installed capacity of the HP has increased, while the capacities of GB and ABS have decreased. This configuration heavily relies on electricity from the electric grid (355,920 kWh/yr), while there is virtually no consumption of natural gas (124 kWh/yr); also, a part of the electricity produced (9348 kWh/yr) is sold to the grid. It is interesting to note that all roof top area is used for the installation of PV and ST, which suggests that it could be interesting to increase its availability. Moreover, compared with the optimal annual cost solution, there was a significant shift in the use of thermal energy storage, from 39.9 kWh of TSR to 314.0 kWh/yr of TSQ. Looking at the annual investment cost, 30% is due to

the installation of ST, followed by the HP with 28%, and the PV with 26%. In the case of the annual CO_2 emissions relative to the manufacturing of each device, the three highest contributions are 52% PV, 18% TSQ, and 17% HP.

The optimal CO_2 emissions configuration presents a total annual cost 31% higher than the optimal annual cost solution, while CO_2 emissions are 52% lower. The shift towards a more environmentally sound configuration incurs an increase of 183% in the annual fixed cost and 354% in the annual CO_2 emissions relative to the manufacturing of the equipment. These are offset by a better energy usage during the operation of the system, translated into a decrease of 29% in the annual operation costs and 59% in annual CO_2 emissions relative to the operation of the system.

Analyzing the annual operation of the optimal annual cost solution, the GE, GB, HP, and TSQ operate all year round, the TSR operates all summer, and the ABS operates from July to September. Of the total electricity consumed, 8.4% is produced by the GE and the rest is purchased from the electric grid. Regarding the heat production, the HP and the GB are the major producers, with 48.4% and 38.6%, respectively. The produced cooling comes almost entirely from the HP (91.7%), being the ABS responsible for supplying peak demands in July and August. Considering the total cooling produced by the system, 4.5% is stored.

Focusing on the optimal CO_2 emissions solution, the HP operates all year except for May, the ABS operates all summer except for September, and the TSQ is used all year round. The GB operates marginally in June to attend heat peak demands. It is worth mentioning that there is dissipation of heat from the ST Q_{stl} in May (4977 kWh/yr). The PV panels account for 23.6% of the electricity consumed, while the rest is purchased from the grid. Of the total electricity produced by the PV, 8.7% is sold to the grid, generating economic benefits. The HP is responsible for 76.2% of the heat produced by the system, followed by the ST with 23.8%; the GB has a negligible share. Of the total heat produced, 26.7% is stored in the TSQ. Cooling is produced mostly in the HP (87.9%) and the rest is covered by the ABS with solar heat from the ST.

The optimization model also determines the hourly operation of the system for each representative day. As an example, Fig. 3 presents, for the optimal annual cost solution, the hourly productions of (a) electricity, in the month of January, (b) heating, in the month of January, and (c) cooling, in the month of July.

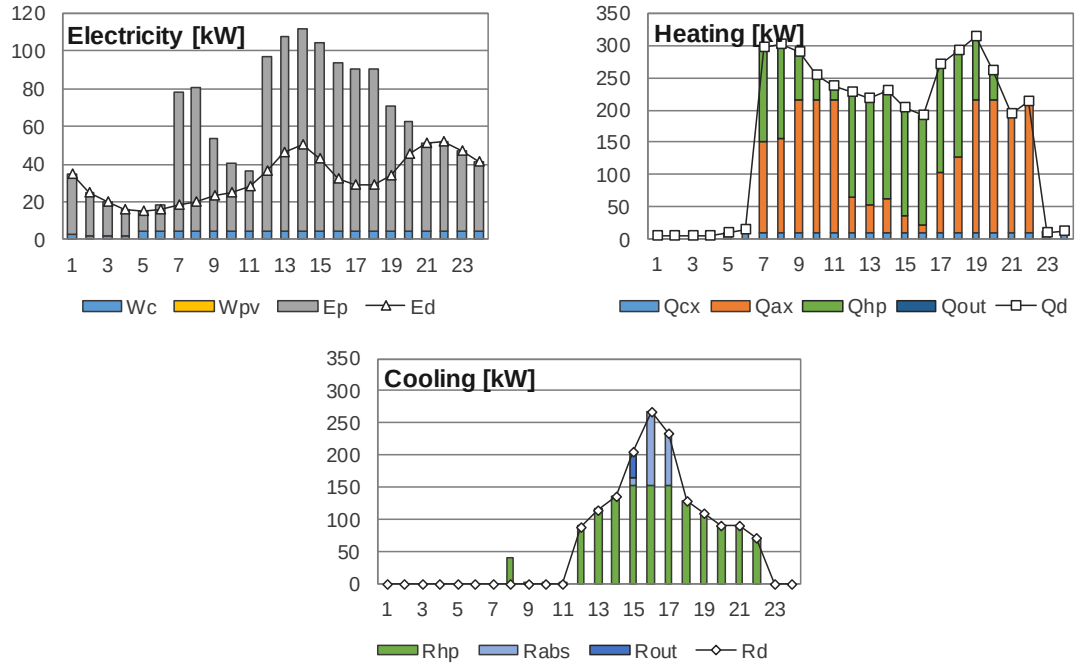

Fig. 3: Hourly production for a representative day of (a) electricity in January, (b) heating in January and (c) cooling in July. Optimal annual cost configuration

In January, only electricity E_d and heating Q_d are required by the consumer center. As can be seen from Fig. 3, the GE operates all through the day producing electricity W_c and heat Q_{cx}; particularly, between hours 6 and 24,

it operates at full load. Also, electricity is purchased from the grid E_p throughout the day. It is interesting to note the increase in the purchase of electricity at hours 7 and 8, which are the last two hours of off-peak rate. Apart from the electricity demand E_d, electricity is consumed by the HP from hour 6 to 20 for heat production Q_{hp}. The HP's load increases in the afternoon, after hour 11; it also complements heat production when the GB is at full load, e.g. hours 9 to 11 and 19 to 20. As already mentioned, the TSQ is used but with negligible shares.

In the month of July, cooling is required from hour 12 to 22. However, as presents Fig. 3, cooling production begins earlier in the day (e.g. hour 8), being stored in the TSR for later use. The ABS operates marginally with heat from the GB at hours 12 and 13, and more significantly from hour 15 to 17, when the HP is at full load. The TSR has one significant charge at hour 8 and one significant discharge at hour 15.

5. Multiobjective optimization

The issue is that economic costs and environmental concern are generally conflicting objectives, which means that the optimal solution for one is not the best for the other, as was demonstrated in Section 4. Multiobjective optimization is used to optimize a problem with two or more conflicting objectives, identifying trade-off solutions among them. These trade-off solutions, also known as non-dominated solutions, constitute the Pareto set, in which no improvement in one objective can be achieved without sacrificing the other (Andiappan, 2017).

Pareto optimization has been extensively applied in the literature concerned with multicriteria problems and many methods are available for solving multiobjective optimization problems. Some methods involve converting the multiobjective problem into a series of single optimization problems. An important question is the role of the decision maker in the procedure. In this regard, *a posteriori* methods for generating Pareto-optimal solutions are preferred. Among them, the ε-constraint has been applied by various authors to the optimization of energy supply systems (Buoro et al., 2013; Carvalho et al., 2012; Fazlollahy et al., 2012; Gebreslassie et al., 2012). In this approach, the problem is optimized with respect to one of the objective functions, while upper/lower bounds are set for the rest of the objective functions. The problem is repeatedly solved for different ε values, obtaining the different trade-off solutions that compose the Pareto set. Based on the Pareto curve obtained, the decision maker has more flexibility to judge the different trade-off solutions and make a more informed decision.

In this paper, the optimization model was solved for the total annual cost objective, subject to CO_2 emissions constraints. The Pareto set obtained is limited by Lim_{sup} = 155,066 ton CO_2/yr (optimal annual cost solution) and Lim_{inf} = 74,240 ton CO_2/yr (optimal annual CO_2 emissions solution). The interval between superior and inferior limits have been subdivided and the model was repeatedly solved. Table 5 presents the ε values considered in the analysis, starting from the optimal annual cost solution (point B), towards the optimal annual CO_2 emissions solution (point A). Along the Pareto curve, different solutions are obtained with different configurations and installed capacities. Fig. 4 shows the Pareto curve obtained, in which equal symbols represent the same configuration (with different installed capacities). As can be seen from Table 5, a total of 33 ε values were evaluated, obtaining 9 different configurations.

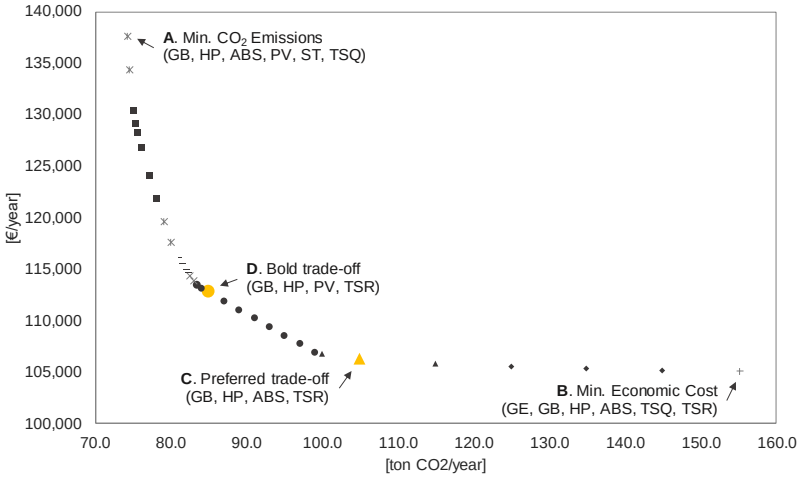

Fig. 4: Pareto curve – Annual economic cost vs. annual CO_2 emissions

Table 5: Trade-off solutions obtained with the ε-constraint method considering economic cost and CO_2 emissions

	ε-CO_2 emissions [tonCO_2/yr]	Economic cost [€/yr]	Installed capacities								Marginal cost [€/tonCO_2]	Average cost [€/tonCO_2]
			GE	GB	HP	ABS	PV	ST	TSQ	TSR		
(**B**)	155.1	105,067	4.2	204.8	162.1	94.0	-	-	0.4	39.9	-	-
	145.0	105,126	3.5	193.5	176.8	83.8	-	-	-	40.0	5.9	5.9
	135.0	105,254	3.1	171.6	201.9	66.3	-	-	-	40.2	12.8	9.3
	125.0	105,453	1.1	169.0	209.8	60.9	-	-	-	40.2	19.9	12.8
	115.0	105,771	-	163.6	218.7	54.7	-	-	-	40.3	31.9	17.6
(**C**)	105.0	106,266	-	140.0	244.6	36.7	-	-	-	40.4	49.5	24.0
	100.0	106,690	-	113.6	273.6	16.6	-	-	-	40.6	84.7	29.5
	99.0	106,916	-	91.8	297.6	-	1.5	-	-	40.7	226.6	33.0
	97.0	107,745	-	91.8	297.6	-	88.1	-	-	40.7	414.4	46.1
	95.0	108,574	-	91.8	297.6	-	174.7	-	-	40.7	414.4	58.4
	93.0	109,403	-	91.8	297.6	-	261.3	-	-	40.7	414.4	69.9
	91.0	110,232	-	91.8	297.6	-	347.9	-	-	40.7	414.4	80.6
	89.0	111,060	-	91.8	297.6	-	434.4	-	-	40.7	414.4	90.7
	87.0	111,889	-	91.8	297.6	-	521.0	-	-	40.7	414.4	100.2
(**D**)	85.0	112,718	-	91.8	297.6	-	607.6	-	-	40.7	414.4	109.2
	84.0	113,170	-	86.6	303.3	-	640.0	-	-	35.3	452.0	114.0
	83.5	113,472	-	75.3	315.6	-	640.0	-	-	23.6	604.3	117.4
	83.0	113,932	-	74.5	316.6	-	634.9	7.1	-	22.7	919.2	123.0
	82.5	114,392	-	74.5	316.6	-	629.4	14.6	-	22.7	920.5	128.5
	82.3	114,631	-	72.6	316.6	-	626.8	18.2	1.9	22.7	953.8	131.3
	82.0	114,884	-	69.7	317.3	-	624.5	21.4	4.8	22.0	1012.7	134.4
	81.5	115,424	-	63.2	320.9	-	620.3	27.1	11.4	18.6	1080.2	140.8
	81.0	116,005	-	59.8	320.8	0.4	615.0	34.5	18.5	18.1	1163.3	147.7
	80.0	117,605	-	56.1	312.6	19.2	603.9	49.7	43.1	-	1599.3	167.0
	79.0	119,643	-	55.8	296.4	30.4	589.2	70.0	89.4	-	2038.6	191.6
	78.0	121,862	-	55.6	285.2	37.4	570.5	95.8	121.1	0.9	2218.4	217.9
	77.0	124,221	-	54.7	267.8	39.3	552.9	120.0	172.6	14.8	2359.3	245.4
	76.0	126,850	-	52.9	260.4	41.4	530.4	151.1	201.1	19.0	2629.2	275.5
	75.5	128,282	-	52.8	253.2	42.7	520.2	165.1	228.8	24.0	2863.0	291.8
	75.3	129,301	-	62.7	265.0	47.8	519.3	166.3	231.0	5.8	4076.3	303.6
	75.0	130,498	-	63.0	269.6	48.8	513.4	174.5	247.2	-	4789.6	317.6
	74.5	134,365	-	54.3	269.6	48.8	480.2	220.2	267.0	-	7734.3	363.7
(**A**)	74.2	137,630	-	49.3	269.6	48.8	461.2	246.5	314.0	-	12,562.0	402.9

The graphs in Fig. 5 show the installed capacities of each technology along the Pareto curve, from the optimal annual cost to the optimal annual CO_2 emissions solution. The analysis of the trade-off solutions that constitute the Pareto curve obtained shows that each technology was included in at least one configuration; on the other hand, no configuration included all eight technologies simultaneously. The GB and the HP were included in all solutions obtained and the TSR was included in most solutions. From the optimal annual cost configuration (B), as CO_2 emissions are forced down towards the environmental optimal (A), there is a shift in the installed capacities of GB and HP: the former decreases, while the latter generally increases. GE is only included at CO_2 levels higher than 125 ton CO_2/yr, and even so with relatively small installed capacities. For total annual emissions below 99 ton CO_2/yr, PV panels begin to be incorporated. ST collectors are included at even lower overall emissions levels, 83 ton CO_2/yr, closely followed by the TSQ at 82.25 ton CO_2/yr. There are two different ranges in which the ABS is included: for CO_2 levels higher than 100 ton CO_2/yr and lower than 91 ton CO_2/yr. It is interesting to look into the role the ABS plays in each scenario: at the higher CO_2 emissions range, the ABS is driven with heat produced with natural gas (Q_{cr} and mostly Q_{ar}); on the other hand, at the lower range, the ABS is driven exclusively with heat from the ST (Q_{str}). It is worth noting that GE was not included in any solution simultaneously with PV and/or ST.

From the analysis of the trade-off solutions obtained, point C in Fig. 4 and Table 5 was selected as preferred intermediate solution because of its good trade-off between both criteria: it achieves a 32.3% reduction in CO_2 emissions with an increase of only 1.1% in costs relative to the optimal cost configuration (B). Moreover, solution C includes only GB, HP, ABS, and TSR. Compared with the optimal annual cost solution (A), there is a

reduction in the installed capacities of GB and ABS and an increase in the installed capacity of HP. As a result, the system consumes 75.7% less natural gas and purchases 31.4% more electricity from the electric grid. By supporting a higher sacrifice for the economic objective, point D in Fig. 4 and Table 5 can also be identified as an interesting trade-off solution: it achieves a 45.2% decrease in CO_2 emissions with an increase of 7.3% in costs relative to the optimal cost configuration (B). The configuration includes GB, HP, PV, and TSR.

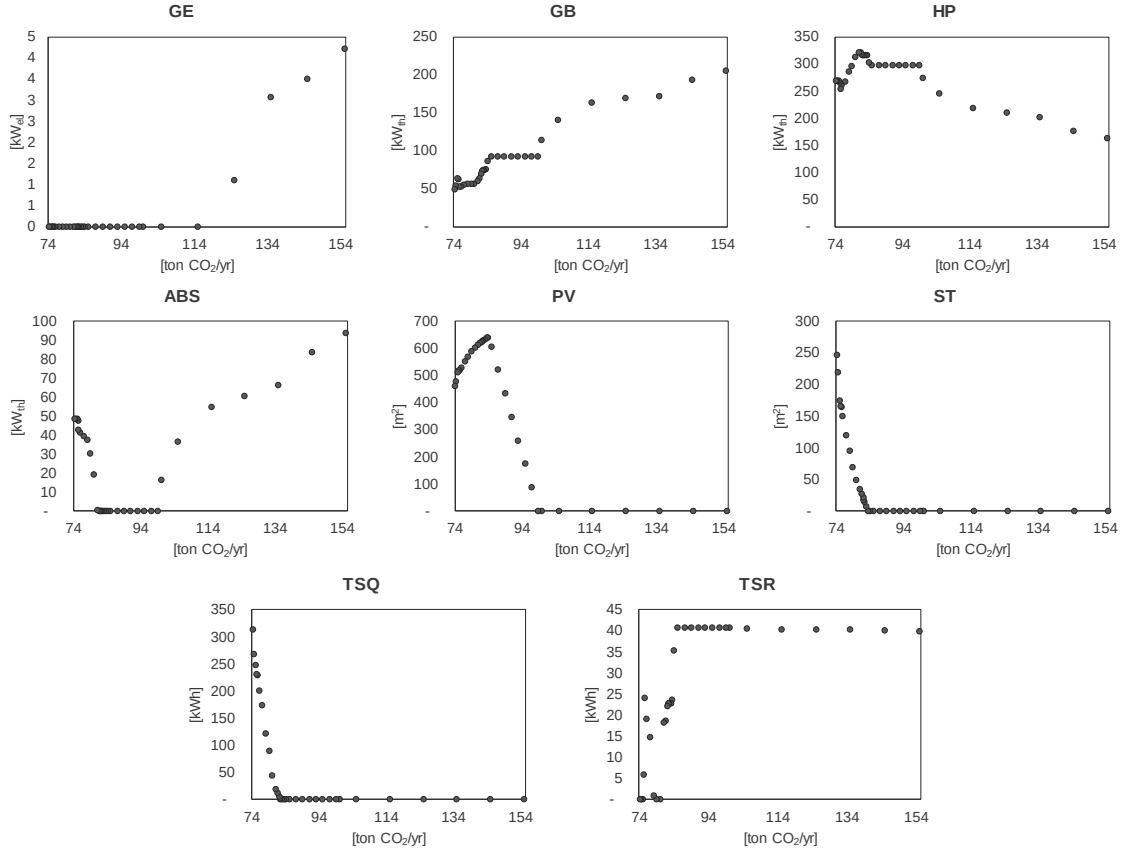

Fig. 5: Installed capacities along the Pareto curve

Table 5 also presents the marginal and average costs of each solution, in €/ton CO_2. The marginal cost represents the cost of moving from one solution to the next in the Pareto curve, while the average cost represents the cost of moving from the optimal annual cost solution (B) to any other. These could be interesting indices to measure the effort the decision maker is willing to make in order to move towards a more environmentally sound configuration. As can be seen from Table 5, it is no surprise that both the marginal and the average costs increase as the system shifts towards more environmentally sound configurations. Moving from one optimum to the other (B → A) involves an average cost of 402.9 €/ton CO_2. However, taking the trade-off solution C into account, the average cost of moving from B to C is only 24.0 €/ton CO_2.

Based on the different circumstances under which the system operates, for instance local subsidies for CO_2 emissions savings and/or stock market prices of CO_2 emissions, the marginal cost could be used to select among the various trade-off solutions obtained. Solution C presents a marginal cost of 49.5 €/ton CO_2. Ensuring a higher economic compensation for CO_2 emissions savings would enable other solutions to be chosen, such as solution D with 414.4 €/ton CO_2.

6. Conclusions

This paper tackled the issue of conflicting objectives in the synthesis of trigeneration systems including renewable energy technologies and thermal energy storage. A MILP model was developed using the optimization software LINGO including two objective functions: minimize the total annual cost and minimize the total annual CO_2 emissions. Both objectives take into account a fixed term, relative to the manufacturing and

installation of the equipment, and a variable term, relative to the hourly operation of the system. The model was applied to a multifamily building located in Zaragoza, Spain.

At first, the objective functions were minimized separately, obtaining the optimal annual cost solution and the optimal annual CO_2 emissions solution. The optimal solutions presented fundamentally different configurations: the optimal cost configuration included cogeneration, whereas the optimal CO_2 emissions configuration included renewable energy technologies. Then, the ε-constraint approach was employed to identify the intermediate trade-off solutions that compose the Pareto curve. As a result, it was possible to identify trade-off solutions that were close to the single-objective solutions with reasonable sacrifices for both objectives; for example, the preferred trade-off solution selected in this study achieved a 46.2% reduction in total annual CO_2 emissions with only an 8% increase in total annual cost relative to the optimal annual cost configuration. This procedure demonstrated the importance of the decision maker in evaluating the trade-off solutions in search for the configuration that best suits the objectives of the analysis.

In the synthesis of energy systems, the quality of the data used plays a central role because it directly affects the results of the optimization model. However, in multiobjective optimization problems, it is essential to maintain all objective functions at the same level of detail. This issue was highlighted in a previous paper by Pina et al. (2017), in which the price of the electricity from the grid and the associated CO_2 emissions were considered constant throughout the year. The present paper improved the optimization model proposed in that work by incorporating hourly electricity prices and CO_2 emissions per kWh, for each representative day. As a result, it was shown that the system takes advantage of the different electricity prices and emissions at different hourly periods to achieve more interesting results in accordance with the objective function.

It is also important to maintain the closest level of detail as possible with regard to the elaboration of the optimization model. For example, it is known that the electricity tariff is generally composed of a power term and an energy term; however, what would be the appropriate counterpart to the power term for CO_2 emissions? Due to the lack of an appropriate value, the authors opted to consider only the energy term in the calculations. Nevertheless, we do recognize having applied an amortization and maintenance factor over the operational lifetime of the system with no equivalent in the CO_2 emissions objective function. These issues should be explored in further studies.

Further work could explore the interconnection with the electric grid, considering local policies on the permission to sell/inject electricity to the grid and its effects on the optimal configuration and operation of the system. Moreover, more technologies could be included in the superstructure, namely prime movers (e.g. microturbines, fuel cell), RES (e.g. wind power, biomass), and energy storage units (e.g. electrical batteries).

7. Acknowledgements

This work was developed in the frame of the research project ENE2014-57262-R, partially funded by the Spanish Government (Energy Program), the Government of Aragon (Spain) and the EU Social Fund (FEDER Program). Eduardo Pina acknowledges financial support from the Brazilian Federal Government and CNPq Science Without Borders Program.

8. References

Andiappan V. State-Of-The-Art Review of Mathematical Optimisation Approaches for Synthesis of Energy Systems. Process Integration Optimization Sustainability. Published Online 13 August 2017. (doi:10.1007/s41660-017-0013-2).

Buoro D, Casisi M, De Nardi A, Pinamonti P, Reini M. Multicriteria optimization of a distributed energy supply system for an industrial area. Energy 2013; 58:128–137.

Carvalho M. Thermoeconomic and environmental analyses for the synthesis of polygeneration systems in the residential-commercial sector. PhD Thesis, University of Zaragoza, 2011.

Carvalho M, Lozano MA, Serra LM. Multicriteria synthesis of trigeneration systems considering economic and environmental aspects. Appl. Energy 2012; 91:245–254.

EDP, 2017. Gas and Electricity Prices - Liberalized Market [WWW Document]. Gas Electr. Prices - Lib. Mark. URL http://www.edpenergia.es/es/hogares/gas-y-electricidad/precios/mercado-libre/ (accessed 8.31.17).

Fazlollahi S, Mandel P, Becker G, Maréchal F. Methods for multi-objective investment and operating optimization of complex energy systems. Energy 2012; 45:12-22.

Gebreslassie BH, Guillén-Gosálbez G, Jiménez L, Boer D. Solar assisted absorption cooling cycles for reduction of global warming: A multi-objective optimization approach. Sol. Energy 2012; 86:2083–2094.

Guadalfajara M. Economic and environmental analysis of central solar heating plants with seasonal storage for the residential sector. PhD Thesis, University of Zaragoza, 2016.

IDAE, 2014. Factores de emisión de CO_2 y coeficientes de paso a energía primaria de diferentes fuentes de energía final consumidas en el sector de edificios en España.

Ito M, Komoto K, Kurokawa K. A comparative LCA study on potential of very-large scale PV systems in Gobi desert. Conf. Rec. IEEE Photovolt. Spec. Conf. 000729–000732, 2009.

Iyer RR, Grossmann IE. Synthesis and operational planning of utility systems for multiperiod operation. Computers and Chemical Engineering 1998; 22:979–93.

Liu M, Shi Y, Fang F. Combined cooling, heating and power systems: A survey. Renew. Sustain. Energy Rev. 2014; 35:1–22.

Lozano MA, Ramos JC, Carvalho M, Serra LM. Structure optimization of energy supply systems in tertiary sector buildings. Energy and Buildings 2009; 41:1063-1075.

Lozano MA, Ramos JC, Serra LM. Cost optimization of the design of CHCP systems under legal constraints. Energy 2010, 35:794- 805.

Mancarella P. MES (multi-energy systems): An overview of concepts and evaluation models. Energy 2014; 65: 1–17.

Pina EA, Lozano MA, Serra LM. Multicriteria synthesis of trigeneration systems assisted with renewable energy sources and thermal energy storage. ASME Paper POWER-ICOPE2017-3103, 10 pages, 2017. (doi:10.1115/POWER-ICOPE2017-3103).

Raluy RG, Serra LM, Guadalfajara M, Lozano MA. Life cycle assessment of central solar heating plants with seasonal storage. Energy Procedia 2014; 48:966-976.

Ramos JC. Optimización del diseño y operación de sistemas de cogeneración para el sector residencial comercial. PhD Thesis, University of Zaragoza, 2012.

REE, 2017. Demanda y producción en tiempo real [WWW Document]. Demanda y Prod. URL http://www.ree.es/es/actividades/demanda-y-produccion-en-tiempo-real (accessed 8.31.17).

Rong A, Su Y. Polygeneration systems in buildings: A survey on optimization approaches. Energy and Buildings 2017; 151:439–454.

Schrage L. Optimization modeling with LINGO. Lindo Systems, 1999.

Serra LM, Lozano MA, Ramos J, Ensinas AV, Nebra SA. Polygeneration and efficient use of natural resources. Energy 2009; 34:575–586.

Wakui T, Kawayoshi H, Yokoyama R. Optimal structural design of residential power and heat supply devices in consideration of operational and capital recovery constraints. Appl. Energy 2016; 163:118–133.

Yokoyama R, Shinano Y, Taniguchi S, Ohkura M, Wakui T. Optimization of energy supply systems by MILP branch and bound method in consideration of hierarchical relationship between design and operation. Energy Conversion and Management 2015; 92:92–104.